Nuclear Materials and Energy 27 (2021) 100987

Contents lists available at ScienceDirect

Nuclear Materials and Energy

journal homepage: www.elsevier.com/locate/nme

The impact of surface morphology on the erosion of metallic surfaces – Modelling with the 3D Monte-Carlo code ERO2.0

A. Eksaeva [a,*], D. Borodin [a], J. Romazanov [a,e], A. Kirschner [a], A. Kreter [a], B.Göths [a], M. Rasinski [a], B. Unterberg [a], S. Brezinsek [a], Ch. Linsmeier [a], E.Vassallo [b], M. Passoni [b,c], D. Dellasega [b,c], M. Sala [c], F. Romeo [c], I. Borodkina [d]

[a] Forschungszentrum Jülich GmbH, Institut für Energie- und Klimaforschung – Plasmaphysik, Partner of the Trilateral Euregio Cluster (TEC), Jülich, Germany
[b] Istituto per la Scienza e Tecnologia dei Plasmi, CNR, Milano, Italy
[c] Dipartimento di Energia, Politecnico di Milano, Via Ponzio 34/3, 20133 Milan, Italy
[d] Institute of Plasma Physics of the CAS, Za Slovankou 3, Prague 8, Czech Republic
[e] ARA-HPC, Jülich Supercomputing Centre, Forschungszentrum Jülich GmbH, Jülich, Germany

A B S T R A C T

The roughness of metallic surfaces has a vital impact on the erosion of plasma-facing materials. Roughness determines the effective sputtering yield Y_{eff} of the facing material. The angular/energy distribution of sputtered particles, and the spatial erosion and deposition distribution. The model for simulation the effect of the surface roughness was earlier implemented into the 3D Monte-Carlo code ERO2.0 and validated using results of ion beam experiments and experiments in the linear plasma device PSI-2. In the present study the developed ERO2.0 surface morphology model was applied to the JET-ILW tungsten (W) divertor consisting of smooth bulk W and W-coated CFC components. Influence of the surface roughness on the W erosion as well as on the transport of sputtered material in conditions of inclined magnetic field was investigated. Simulation results are in a good agreement with existing experimental findings.

Introduction

Erosion of plasma-facing components (PFCs) determines their lifetime and affects several plasma-surface interaction (PSI) issues important for ITER [1], like dust formation, tritium (T) co-deposition with beryllium (Be) [2] or plasma dilution due to the material transport [3]. Surface morphology is shown to have a significant effect on sputtering parameters (effective sputtering yield Y_{eff} from the rough surface, velocity distribution of sputtered particles) [4,5], which in turn can affect the transport of sputtered material [6]. Effects like the decrease of the Y_{eff} for non-smooth surfaces, sheath potential distribution modification near the rough surface [7,8,9] as well as surface modification during the plasma irradiation [10] were reproduced using numerical simulation. Tools like the SDTrimSP-3D code can be used to simulate the temporal evolution of regular surface structures under ion beam exposure [11]. Still, most of micro-scale simulations utilize input data (plasma parameters, incident ions distributions) produced by other simulation tools, while codes for transport calculations do not take into account the surface roughness effect when forming velocity distributions of sputtered particles. Developing a reliable model allowing self-consistent simulation of the surface roughness effect on erosion and transport of material in tokamaks is therefore of importance.

The 3D Monte-Carlo code ERO2.0 [12] is a recognized tool for modelling of the PSI and local impurity transport in the plasma. It uses the test particle approximation [13] to simulate movement of impurities in the plasma and considers a wide range of physical processes like ionization, recombination, light emission, plasma friction, elastic collisions, etc. The first version of the code ERO1.0 (no massive parallelization, smaller simulation volume) has been applied to a wide range of experimental devices – from toroidal devices like ITER [13] to linear devices like PSI-2 [6]. ERO2.0 was recently applied for JET ITER-like wall (JET-ILW) [12] and ITER [14] simulations. The massive parallelization provides the possibility to simulate a large number of test particles and the code is capable of processing large and complex 3D surface geometries. In our previous studies [15,16] the surface morphology model was implemented into the ERO2.0 code, which assumed the smooth surface of PFCs before. The model was applied to several numerically-generated surface topographies, tested on existing results of ion beam experiments [11] and validated in experiments in the PSI-2 linear plasma device. A good agreement between simulations and experiments was observed in all validation cases.

With respect to PFCs of large toroidal devices one can define surface

* Corresponding author.
E-mail address: a.eksaeva@fz-juelich.de (A. Eksaeva).

https://doi.org/10.1016/j.nme.2021.100987
Received 5 September 2020; Accepted 24 March 2021
Available online 30 March 2021

as rough if its value of the surface roughness (R_a – average peak height of structures on the surface) is of the order of 10 μm and smooth if it is reaching ~1 μm. Therefore most of simulations presented in this paper are done in a micro-scale simulation volume for structures of ~10 μm scale. To extract information about influence of the surface roughness on the transport of sputtered material, simulations on the micrometer-scale should be combined with ERO2.0 modelling on the machine-scale. For that effective sputtering parameters (Y_{eff}, velocity distributions of sputtered particles) of the rough surface can be derived from micrometer-scale calculations and used as an input for the machine-scale simulations. In turn, information on incident on the surface impurity and plasma particles obtained in machine-scale simulations can be used as an input for micro-scale cases. In the present study the developed ERO2.0 surface morphology model is applied to the JET-ILW W divertor using the multi-scale modeling. The main difference to previous validation cases is the highly-oblique magnetic field at the surface. It leads to the shadowing of some surface areas by neighboring structures and different distribution of incident plasma ion angles in comparison to the normal incidence case. The aim of the study is to estimate which effect surface roughness can have on the sputtering parameters and on the transport of the sputtered material in the divertor of the JET-ILW tokamak. Areas of preferential deposition and erosion on the surface are analyzed and comparison to available experimental results is provided.

ERO2.0 surface morphology model

Model description

In the ERO2.0 surface morphology model the rough surface is represented by a polygon mesh of surface cells. For each individual cell the sputtering yield and the angular distribution of sputtered particles are calculated using the local incidence angle of the plasma flux constant within the cell (the cell is assumed flat and smooth). For each cell the amount of sputtered atoms is calculated and distributed between "test particles" (super-particle, consisting of many "real" atoms), which are traced later on by ERO2.0. They are traced in the local plasma volume near the rough surface until they escape it or hit neighboring structures. Particles finally escaped from the surface define effective sputtering parameters of the rough surface and take part in the material transport on the macro-scale (or machine-scale). This interaction of micro- and macro-scale simulation steps is depicted in Fig. 1.

Various rough surface topographies can be constructed in ERO2.0: the surface relief can be defined by a formula or be randomly generated

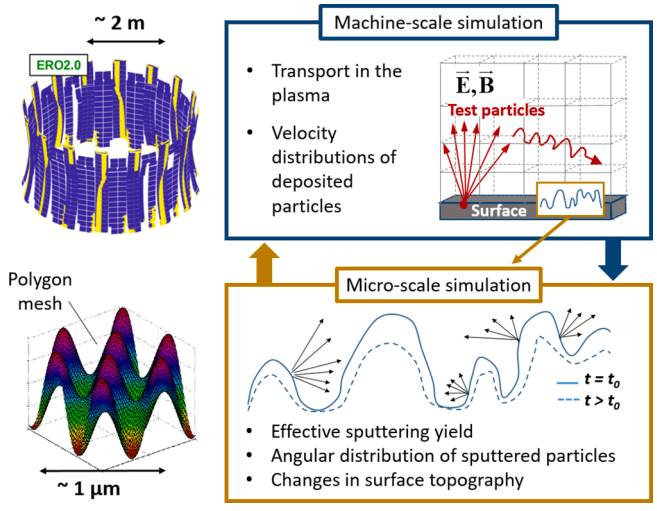

Fig. 1. Scheme of interaction between micro-scale and machine-scale simulations.

using the certain fractal dimension value D_{fract}. Alternatively, realistic topographies based on Atomic Force Microscopy (AFM) [17] measurements can be used (for surfaces with lower value of R_a, $R_a <\approx 1$ μm). The local angle of the surface normal with the magnetic field can vary significantly along the rough surface affecting the angular and energy distributions of sputtered particles on the slopes of rough surface structures [18]. Angular and energy distributions of sputtered particles at each point of the surface are calculated using results of SDTrimSP code simulations [19]. Sputtering yields as well as energy and angular distributions of sputtered particles are resolved by the incident ion energy E_{in} and angle α and presented in the tabular form or using the Eckstein analytic fit formula [20].

Temporal evolution of surface structures under continuous plasma irradiation can be simulated using the model as well. From the calculated amount of sputtered/deposited material for each surface cell, the thickness of sputtered/deposited layer is defined (sputtering bringing a negative contribution and deposition - a positive one). For every vertex a weighted average of sputtered thickness values from all its neighboring faces is then calculated. The unity vector of the shift direction is estimated as a weighted average of neighboring faces normal vectors. After that normals and areas of all surface cells are recalculated based on new vertex positions. Finally, the smoothing procedure – position of each vertex is replaced with the average of positions of eight neighboring vertices - is applied.

Model validation

In our first study [15] the influence of various artificially-generated rough surfaces on sputtering parameters was investigated under the assumption of a normal plasma impact. For the two considered rough surface topographies the decrease of the Y_{eff} by up to the factor of ≈2–5 was observed with the increase of the aspect ratio of structures. To validate the surface modification algorithm in the code, results of recently conducted ion beam experiments [11] were utilized. These experiments exclude typical for the plasma irradiation processes like the sheath E-field and velocity distributions of incident ions, but concentrate on the physical sputtering itself. Validation of the model was successful and and the model could correctly reproduce the experimentally observed modification of the surface with the irradiation as described in our previous study [16].

Finally, the model was validated under plasma irradiation in the PSI-2 linear plasma device [21]. The device provides versatile opportunities for PSI processes investigations: mass loss measurements at the target can provide the information about the net erosion, while the optical spectroscopy measurements near the target surface can help to estimate the gross erosion and give an insight in transport properties [6]. Dedicated experiments in PSI-2 linear plasma device using molybdenum (Mo) samples of different pre-defined roughness values [22] have confirmed that increase of the surface roughness value from $R_a < 20$ nm up to $R_a = 600$ nm leads to the suppression of erosion by ≈ 40% [16]. ERO2.0 simulations using the developed model and AFM measurements of the rough samples utilized for PSI-2 experiments reproduce the observed decrease of the sputtering yield with the increase of the surface roughness value [23].

Applying the model for the JET-ILW divertor

Set-up of micro- and macro-scale simulations

To reveal possible changes in sputtering yields and angular distributions of sputtered W particles due to the surface roughness the developed model was applied for the JET-ILW divertor Tile 5 (bulk W)/ Tile 6 (rough W-coated CFC) [1] outer strike point (OSP) conditions. The OSP determines the maximum of the incident flux (and thus sputtering) and its position can vary significantly between various discharges or even during a single pulse being both at Tile 5 and at the neighboring

Tile 6 (see Fig. 2a).

The main difference between Tile 5 and Tile 6 of the JET-ILW divertor is that Tile 5 consists of the bulk W while Tile 6 is manufactured of a rough CFC substrate coated by ≈3 μm W layer with a Mo interlayer. Information regarding the W-coated CFC tile's surface roughness and erosion/deposition patterns useful for ERO2.0 simulations is summarized in Fig. 2. In the SEM picture (Fig. 2b) of the Tile 6 cross-section, CFC and W are marked, as well as the Mo interlayer. One can notice three scales of the surface roughness (~10 μm, ~1 μm and <1 μm, marked). In Fig. 2c the schematic view of various roughness scales is presented. In Fig. 2d an illustration for erosion and deposition patterns at W-coated CFC tiles is shown (erosion of the plasma-facing areas, deposition preferably in shadowed areas). In the JET-ILW third campaign 2011–2012 and in years 2001–2004 one could indeed detect the preferable deposition of Be in areas shadowed from the plasma by the surface structures and erosion of plasma-wetted areas [2,24]. The measured value of the surface roughness for Tile 5 surface was $R_a = 2$ μm [25], allowing considering it as relatively smooth in comparison to Tile 6 (roughness ~ 10 μm). Therefore all simulations were done for the W-coated CFC Tile 6 and compared to the smooth case (corresponding to the bulk W Tile 5). In [26] it is shown that even though the Tile 6 in the second JET-ILW campaign was irradiated considerably longer than the Tile 5 (using the same irradiation conditions), similar erosion values have been observed from both tiles and higher roughness of the Tile 6 surface is proposed as a probable reason for this. Therefore estimating the effect of surface roughness on the erosion of the JET-ILW Tile 5/Tile 6 was one of objectives of the present work.

In ERO2.0 simulations on the micro-scale aimed at estimating the surface roughness influence on the erosion and transport of sputtered material, constant and homogeneous magnetic field and plasma parameters have been assumed near the rough surface: $B = 2$ T, $T_e = T_i = 20$ eV, $n_e = 5 \times 10^{19}$ m^{-3} for the inter-ELM phase and $n_e = 1 \times 10^{20}$ m^{-3} for the intra-ELM phase (parameters at the strike point at the bulk W Tile 5 [27], assumed to be similar for the strike point at W-coated CFC Tile 6). Furthermore, since the strike point moves along both tiles during various plasma pulses, simulations for various inclination angles of the magnetic field were of interest. For simulations of erosion of the W-coated CFC (Tile 6) presented in this paper a wide interval 80°-89° was taken. A more thorough description of this study and utilized test cases can be found in [41].

The distribution of the electric field near the surface can be influenced by the surface roughness, therefore understanding the scale of this effect was important for conducted simulations. Analytical estimations of the sheath width near the JET-ILW Tile 5/Tile 6 surface based on [28] have shown that the sheath width is >1 mm for both inter- and intra-ELM conditions for all considered in this study B-field inclination cases (80°–89°). Therefore even the roughness of the largest scale (~10 μm) will not be capable of influencing the sheath potential distribution near the rough surface. Thus the assumption of a homogeneous electric field near the rough surface in ERO2.0 "micro-scale" simulations is valid.

In this study the effect of surface roughness on the erosion was simulated without and with tracing of incident plasma/impurity ions near the rough surface. In the first case pre-calculated sputtering yields averaged over incident ions velocity distributions have been utilized to calculate sputtering from each surface cell, however single energy and angle were assumed for impacting ions (D, Be) to sample velocities of sputtered particles during the simulation. Self-sputtering by re-deposited W was not considered and shadowing of surface structures was calculated based on magnetic field lines. This approach is enough to estimate the influence of the surface roughness on the sputtering yield and angular distributions of sputtered particles in the JET-ILW divertor Tile 5/Tile 6 configuration. In the second case all incident ions (D, Be, W) have been traced near the rough surface. This approach provides more sophisticated shadowing pattern on the rough surface, takes into account erosion by re-deposited W ions and gives the information on distributions of preferential areas of erosion and deposition over the rough surface. In this case simulations on the machine-scale needed to be conducted to provide the information on the re-deposited W flux on the surface.

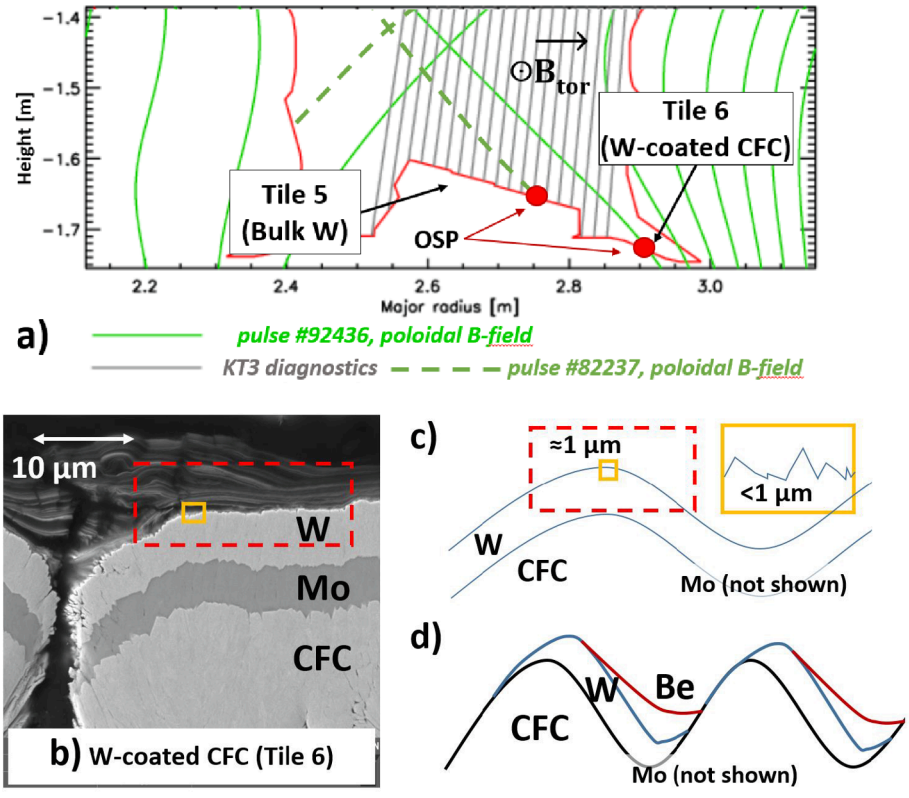

Fig. 2. a) Schematic poloidal view of the JET-ILW divertor with flux surfaces (magnetic field lines lie within these surfaces) from two different plasma pulses and lines of sight of the "KT3" high-resolution optical spectroscopy diagnostics marked. OSP can have a different position depending on the pulse; b) SEM image of the rough surface of CFC W-coated JET divertor tiles before the irradiation [40] with three roughness scales marked; c) Schematic view of the three surface roughness scales observed: ~10 μm, ~1 μm and <1 μm; d) Schematic illustration of the erosion/deposition pattern on CFC W-coated JET divertor tiles (blue line – W surface, red line – deposited Be surface). (For interpretation of the references to color in this figure legend, the reader is referred to the web version of this article.)

It is important to note that using magnetic field lines to calculate shadowing on the rough surface (as it is done in the first approach) is a very crude approximation, even though enough for providing first estimations without large computational effort. Such shadowing model assumes that ions gyro-radius is negligibly small in comparison to shadowed/shadowing structures which is not the case for μm-scale structures. Therefore simulations using tracing of incident ions (explicit shadowing calculation) are indispensable to obtain reliable estimation of the surface roughness effect.

Velocity distributions of incident plasma ions

Tiles of the JET-ILW divertor experience bombardment by both D plasma ions and Be ions originating from the main chamber wall. In Fig. 3 one can see angular distributions of incident D^+, Be^+, Be^{3+} ions for various angles of the B-field with respect to the surface normal (distributions for Be^{2+} and Be^{3+} ions are not depicted for the sake of shortness). Distributions were obtained using the semi-analytical solver from [29] for the smooth surface. The distributions have shown weak dependence on local n_e and T_e and for all ion types they shift to lower angles when the angle between B-field and the surface normal decreases. The energy distribution (Fig. 2d) is a Maxwellian distribution shifted by the value of the sheath potential due to the acceleration of ions there. The high-energy tail of such distribution can cause erosion even if the mean energy is below the sputtering threshold, therefore sputtering yields averaged over many incident angle/energy combinations were calculated in the frame of this work.

In the case when these ions were not traced near the surface during micro-scale simulations, these averaged yields were used to calculated erosion at every surface cell of the surface topography. Nevertheless, as the first approximation, a single angle and energy of incidence were assumed for D and Be ions for generation of sputtered particles velocities distributions in ERO2.0. These angle and energy were taken as their most probable values from distributions in Fig. 3 (e.g. in average 50° incidence for 80° B-field inclination, $E_{in} \approx 500$ eV incidence energy for Be^{4+} when $T_e = 30$ eV). The concentrations of different Be charge states incident on Tile 5 and Tile 6 were assumed to be 0.25% Be^+, 0.18% Be^{2+}, 0.02% Be^{3+} and 0.05% Be^{4+} based on ERO2.0 global migration simulations for the JET-ILW H-mode inter-ELM phase (like in [15]). As a first approximation, these concentration values have been also assumed for the intra-ELM phase.

For the case when ions are explicitly traced near the rough surface it was also important to calculate their velocity distributions at the border of the simulation volume – at ~100 μm distance from the surface. Such simulation were conducted for both inter-ELM and intra-ELM cases. In the case of inter-ELM conditions distributions obtained at 100 μm from the surface looked very close to those presented in Fig. 3. Distributions obtained for intra-ELM conditions are presented in Fig. 7 together with W incident ions distributions obtained using the macro-scale simulation (described in section 3.3). As an input for the analytical solver Maxwellian distribution of plasma ions was assumed at the sheath entrance (for inter-ELM conditions with $T_{mean} = 30$ eV for all ions, for intra-ELM conditions with $T_{mean} = 1$ keV for D ions and $T_{mean} = 4.5$ keV for Be ions as proposed in [27]).

Generated rough surfaces

Based on the surface information for Tile 6 several rough surface shapes for ERO2.0 simulations were generated. Sensitivity scans on various shapes and characteristic sizes of the rough surface structures were conducted. Several examples of generated surface topographies (~10 μm, ~1 μm, <1 μm) are presented in Fig. 4. Two types of generated rough surfaces were used for the tests: a randomly-generated surface determined by a certain fractal dimension (D_{fract} = 2.0–2.9) and an average peaks height (<h> = 4–20 μm, Fig. 4a,b) and a surface consisting of 3D cosine peaks defined by their width ($w = 80$ μm) and height ($h = 15$ and 30 μm) with an option of adding a "second layer" of peaks ($w = 8$ μm, $h = 1.5$ and 3 μm) on the top (Fig. 4c,d).

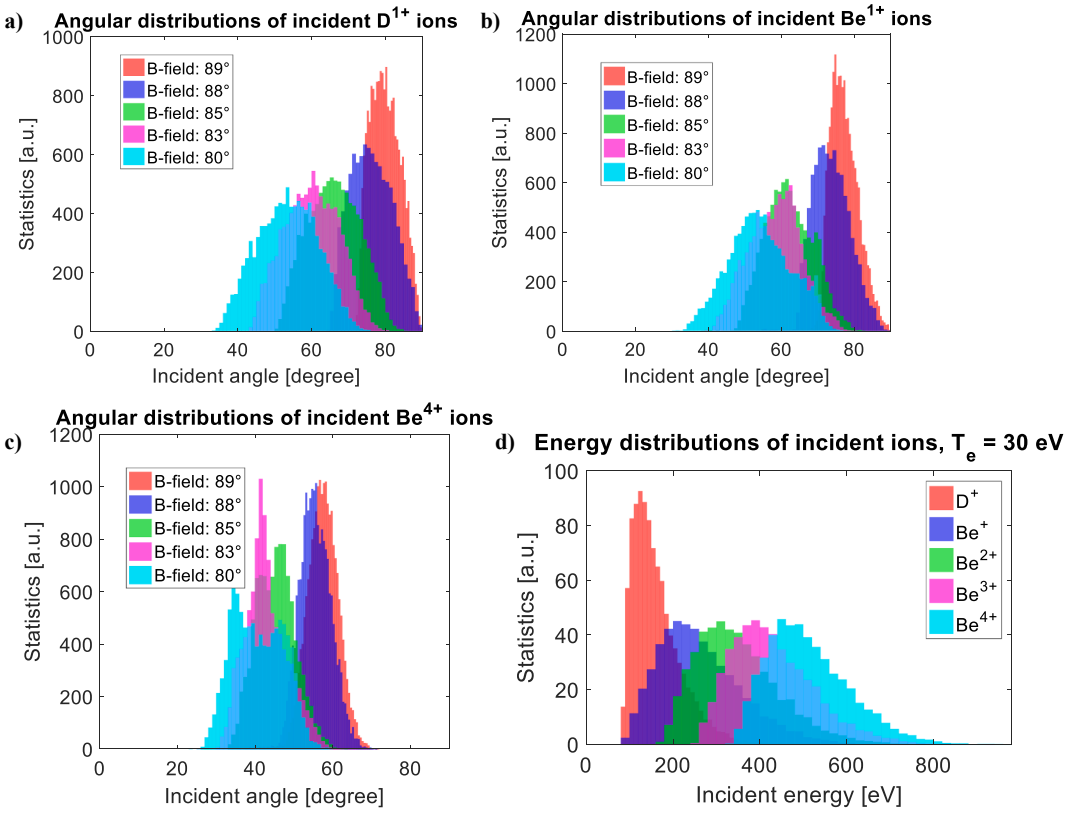

Fig. 3. Angular distributions of incidence on the JET-ILW Tile 5: (a) D^+, (b) Be^+ and (c) Be^{4+} ions, calculated using the analytical approach [28] for angles of the B-field with respect to the surface normal α = 80°, 83°, 85°, 88°, 89°. (f) Energy distributions calculated for incident D^+, Be^+, Be^{2+} and Be^{3+} ions for $T_e = 30$ eV.

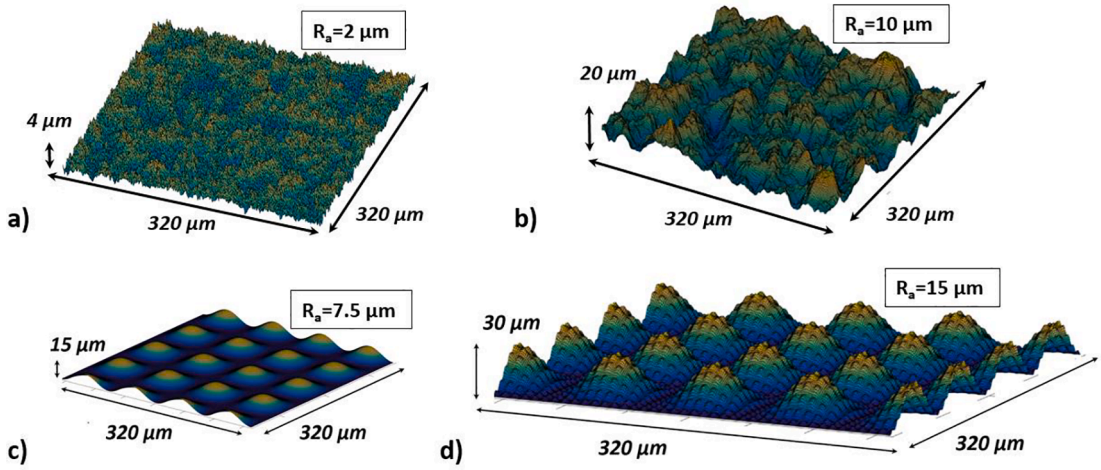

Fig. 4. Examples of generated surfaces. a) Randomly-shaped surface determined by the fractal dimension D and average size of peaks <h> = 4 μm, D = 2.9, b) D = 2.0, <h> = 10 μm; c) surface defined by 3D cosine peaks of h = 15 μm; d) h = 30 μm with 1 μm scale peaks on top.

In the case of the stochastic surface, increasing the fractal dimension D_{fract} can be partially compared to adding new "layers" of the roughness (for example, roughness scale of < 1 μm scale). For the same reason small cosine peaks can be added on the top of large 3D cosine peaks (Fig. 4d). This is plausible for the understanding of the influence of structures of a smaller scale on the erosion or angular distributions of sputtered particles.

Simulation without tracing of incident plasma ions near the rough surface (micro-scale)

ERO2.0 simulation results for the considered surfaces and different inclinations of the B-field when incident ions are not traced near the surface are summarized in Fig. 5. In general, interplay of several factors is determining the resulting value of Y_{eff} and thus the shape of curves in Fig. 5:

- Distribution of local angles of incidence over the plasma-wetted area and angular dependence of averaged plasma sputtering yields for each species (see Fig. 6b,c).
- Relative concentrations of various charge states of incident ions.
- Shadowing produced by surface structures.
- Re-deposition of sputtered material on neighboring structures.

These effects in turn depend on the magnetic field inclination, plasma/wall species combination and surface topography.

Fig. 5a shows the ratio of the effective sputtering yield of the rough surface to that of the smooth one (Y_{eff}/Y_{smooth}) for the case of the randomly-generated surface defined by the fractal dimension value D_{fract}. Two B-field angles are considered: 80° and 89° and three average peaks values $<h>$ = 4 μm, 10 μm, 20 μm. One can notice that higher peaks and higher D_{fract} values lead to a lower sputtering yield Y_{eff}. It is also noticeable that for the magnetic field inclination 80° Y_{eff}. is lower in comparison to the 89° case. This can be explained by the fact that in the second case (89°) only "peaks" of the surface are plasma-wetted, while in the first case (80°) also parts of "valleys" are exposed. Therefore, even though in the case of 80° B-field inclination the effective exposed area and thus total amount of eroded material is higher than in the case of 89° B-field, particles sputtered from "valleys" have a lower probability to "escape" the surface due to deposition on the neighboring structures. Thus, although the absolute amount of eroded particles is higher in the first case, a larger fraction of them escapes the surface (not stopped by neighboring structures) in the second case, leading to in general higher value of Y_{eff}. The lowest value of $Y_{eff}/Y_{smooth} = 0.3$ is observed for the B-

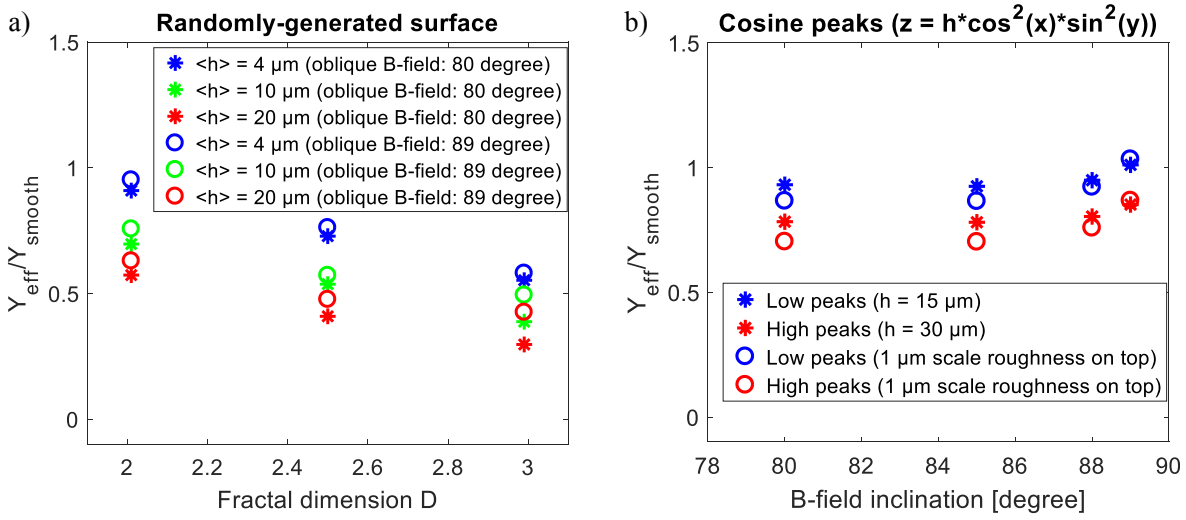

Fig. 5. Ratio of the effective sputtering yield Y_{eff} from the rough surface to the sputtering yield Y_{smooth} from the smooth surface for the case of (a) randomly-generated surface with various fractal dimension values D (two average peaks values $<h>$ = 4 μm, 10 μm, 20 μm) and (b) the surface with 3D cosine peaks (with h = 15 μm and h = 30 μm and with/without 1 μm scale peaks on top). B-field angles are: 80°-89°.

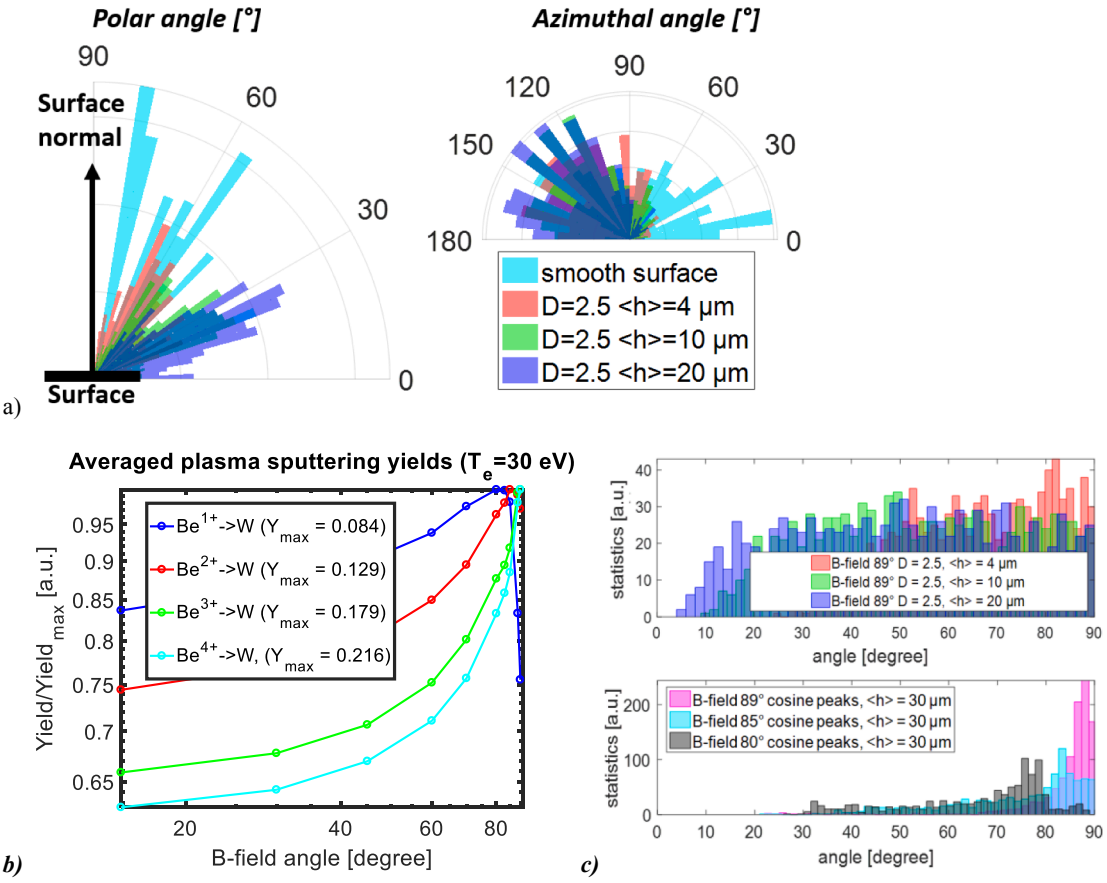

Fig. 6. a) Comparison of the angular distribution of sputtered W from the rough and from the smooth surfaces (example of randomly-formed surface with $D = 2.5$, $<h> = 4$–20 μm, B-field inclination 88°). b) Averaged plasma sputtering yields for W sputtering by Be ions (divided by its maximum value). c) Distributions of local angles between the surface normal and the magnetic field for different rough surface geometries.

field inclination 80°, $D_{fract} = 2.9$ and $<h> = 20$ μm. Such parameters of the surface are however not very realistic for the JET-ILW divertor tiles. The more realistic case would be $D_{fract} = 2.0$–2.5 and $<h> = 10$ μm leading to $Y_{eff}/Y_{smooth} \approx 0.6$ (Fig. 5a).

Angular distributions (polar and azimuthal) of sputtered particles for the randomly-generated surface are shown in Fig. 6a for various heights of the structures. In all the cases the azimuthal distribution is directed in the opposite to the incident direction hemisphere and higher peaks of the rough surface lead to a more "oblique" angular distribution. The first is due to the fact that sputtered particles are emitted in the opposite to the sputtering flux incidence direction, while the second is due to a wider distribution of local incident angles produced by higher peaks. Modification of the angular distribution shown in Fig. 6a is likely to reduce the impurities influx in the plasma from the JET-ILW divertor tiles. In this case neutral sputtered particles travel a smaller distance from the surface before they are ionized, and therefore are more likely to be re-deposited.

In Fig. 5b Y_{eff}/Y_{smooth} is depicted as a function of the B-field lines inclination (80°- 89°) with respect to the surface normal for the case of surface with 3D cosine peaks for peaks height $h = 15$ μm, 30 μm with/without smaller-scale peaks on the top. In general the predicted ratio is $Y_{eff}/Y_{smooth} > 0.6$. For the most realistic case of B-field inclination 88° (was also assumed in [27] for ERO1.0 simulation of the Tile 5 erosion) one obtains $Y_{eff}/Y_{smooth} = 0.75$–$0.90$. Presence of smaller structures on the top only leads to minor variations of the erosion.

The observed shape of the curve can be explained by the interplay of factors listed in the beginning of the section. For example, the small variation of the ratio Y_{eff}/Y_{smooth} between 80° and 85° B-field inclination cases is connected to the fact that the increased plasma-wetted area for the 80° B-field inclination is compensated by the decrease of the plasma-averaged sputtering yields (the local incident angles distribution is shifted in the direction of lower angles for 80° B-field inclination case in comparison to the 85°, while plasma-averaged sputtering yields are in general growing with the B-field angle as shown in Fig. 6b,c). At the same time, for the 89° B-field angle only 10% of the surface is plasma-wetted, but these parts of the surface experience higher erosion, since the distribution of local incident angles of incidence shifts in the direction of higher angles. In general simulations indicate ≈20% higher gross erosion from the rough surface than from the smooth one in considered cases. Finally, 20–30% of sputtered particles are not escaping the surface due to the re-deposition. Interplay of these effects leads to the $Y_{eff}/Y_{smooth} \approx 1$ for the B-field inclination 89° and $Y_{eff}/Y_{smooth} \approx 0.6$–$0.9$ for the B-field inclination 80°.

Angular distributions of sputtered particles from the rough surface defined by regular cosine peaks appeared to be similar to that of the smooth surface. Minor variations have been observed between B-field inclination cases and different surface roughness geometries. Stability of the angular distribution with respect to the surface state in this case can be accounted to the fact that most of the "valleys" are shadowed from the plasma flux and atoms are sputtered only from the "peaks" and therefore their movement is not affected by neighboring structures. This is different to results obtained for the randomly-generated surface due to a much wider distribution of local angles of incidence there (see Fig. 6c).

Obtaining velocity distribution of W re-depositing atoms (macro-scale)

In the first tests incident ions were represented with a single incident angle and energy (extracted from distributions presented in Fig. 3) and

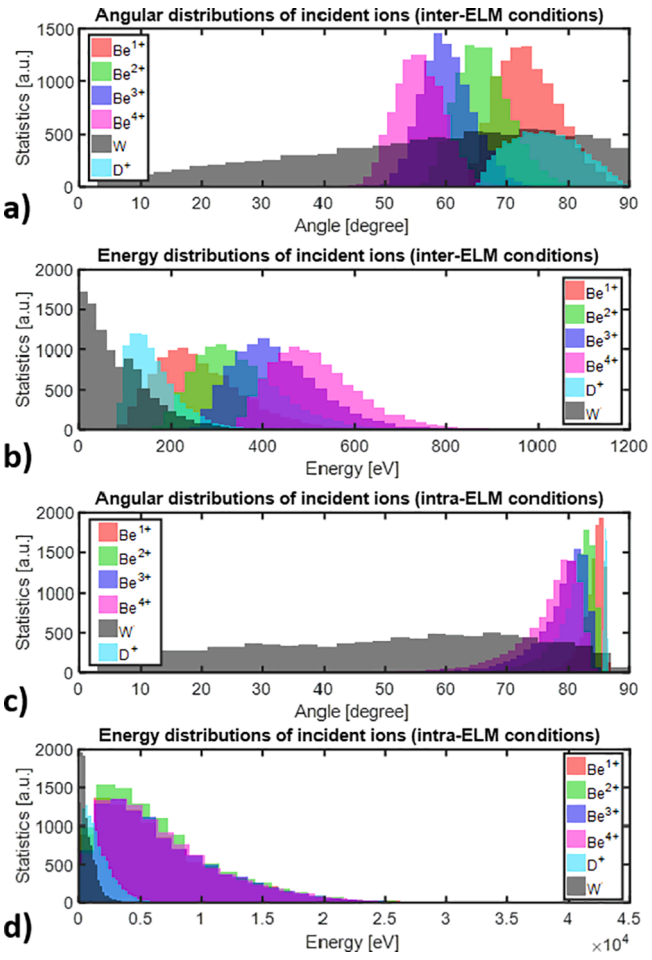

Fig. 7. Angular distributions of ions incident on the surface for (a) inter-ELM and (c) intra-ELM conditions. Energy distributions of incident on the surface ions for (b) inter-ELM and (d) intra-ELM conditions.

only sputtered particles have been traced by ERO2.0. Velocity distributions of plasma ions were taken into account only for calculation of plasma-averaged sputtering yields. Shadowing within the surface was calculated based on magnetic field lines and assuming that plasma ions are moving along them. In order to produce more realistic shadowing patterns on the rough surface, explicit tracing of incident ions near the rough surface is needed. Incident D^+, Be^+, Be^{2+}, Be^{3+}, Be^{4+} ions were traced by ERO2.0 near the rough surface until they collided with the surface structures, forming plasma-wetted and shadowed areas. Two surfaces considered above – regular 3D cosine peaks of $h = 20$ μm with smaller peaks on the top and randomly-generated self-affine surface with $D_{fract} = 2.5$, $<h>=10$ μm – were used to make estimations of the net erosion distribution over the rough surface in both inter- and intra-ELM conditions (areas of erosion and deposition).

The later considered micrometer-scale volume for rough surface calculation is too small to allow tracing of incident ions from the sheath entrance (sheath width 1–3 mm for the configuration at hand), therefore information about angular and energy distributions of plasma and impurity ions when entering the simulation volume should be provided. These distributions were discussed earlier and are presented in Fig. 3 and Fig. 6.

To obtain velocity distributions of W ions entering the volume (re-deposition of sputtered material) simulations on the machine-scale for both inter- and intra-ELM conditions needed to be conducted. It is known that W re-deposition in the JET-ILW divertor is very high and can influence net erosion/deposition zones significantly [30]. Therefore including the W re-deposition flux into the simulation is of high importance. Similar simulations have been already done for the bulk-W Tile 5 in [27], where plasma parameters at the OSP and their decays are proposed. Under the assumption that these parameters are similar for the W-coated CFC tile (Tile 6), macro-scale simulations in the volume 200x200x20 mm^3 were conducted and their results applied for micro-scale modelling of the rough surface later. ERO2.0 simulation (W erosion and its transport near the PFC surface) provided velocities and charge states of re-deposited W particles, which were then used as an input for micro-scale simulations described below. All obtained distributions are depicted in Fig. 7.

Simulation with tracing of incident plasma ions near the rough surface (micro-scale)

In order to reproduce natural shadowing pattern and take into account erosion by redeposited W, simulations using explicit tracing of incident plasma/impurity ions near the rough surface have been conducted. A simulation volume of 400 × 400 × 100 $μm^3$ was considered and incident ions distributions depicted in Fig. 3 and Fig. 4 were used as an input. Net erosion distributions obtained for all considered cases are presented in Fig. 8. One can notice that areas of net erosion are concentrated at the areas "facing" the plasma incidence, while shadowed areas are experiencing net deposition. In Fig. 8e - a copy of Fig. 8b with a scaled on the deposition values color-bar - net deposition areas can be visible. Besides direct deposition of Be from the plasma, also "capturing" of the incident and afterwards reflected Be ions in surface "valleys" contributes to the accumulation of Be deposits there (observed on Tile 6 after the irradiation [24]). For the inter-ELM conditions decrease by ≈20% in the net erosion is observed for the randomly-formed topography (Fig. 8b), while surface with cosine peaks (Fig. 8a) does not lead to the decrease of the net erosion due to the low aspect ratio of surface structures (goes in line with estimations presented in Fig. 5). For intra-ELM conditions decrease by 30–50% is observed for both considered topographies.

Obtained results confirm that the surface roughness is a probable reason for the lower net erosion of the JET-ILW divertor Tile 6 than that of Tile 5 as reported in [24] and that shadowed from the plasma areas experience net deposition, while plasma-wetted parts experience net-erosion. One should note, that reduction of the net erosion value for the rough surface is first of all due to the re-deposition on the micro-scale *within* the surface (considered during micro-scale simulations). For particles, escaped from the surface and returned there later on, re-deposition values reported in the literature (e.g. up to 99% local W re-deposition values on the Tile 5 [27]) stay unchanged, as they are determined by the transport of sputtered material in the plasma and not by the surface topography.

Conclusions

In the frame of this study, a model for simulating the surface roughness effect on the erosion of PFCs and transport of sputtered material developed in previous studies was applied for modelling the effect of surface roughness on sputtering and deposition in the JET-ILW divertor conditions. Examples of regular (cosine peaks) and randomly-formed (determined by the fractal dimension D_{fract}) surface topographies were tested in order to understand influence of the surface roughness on the Y_{eff} and angular distributions of W sputtered from Tile 5/Tile 6 of the JET-ILW divertor. Micro-scale simulations have been conducted without and with tracing of incident plasma/impurity ions near the rough surface.

Simulations without tracing of incident ions have shown that surface roughness leads to a reduction of the effective sputtering yield by up to 50% depending on surface parameters and only the largest scale roughness (Ra > 10 μm) determines the final result. A multi-scale ERO2.0 modelling approach was applied to estimate the effect of the surface roughness as well as to define areas of net erosion and deposition

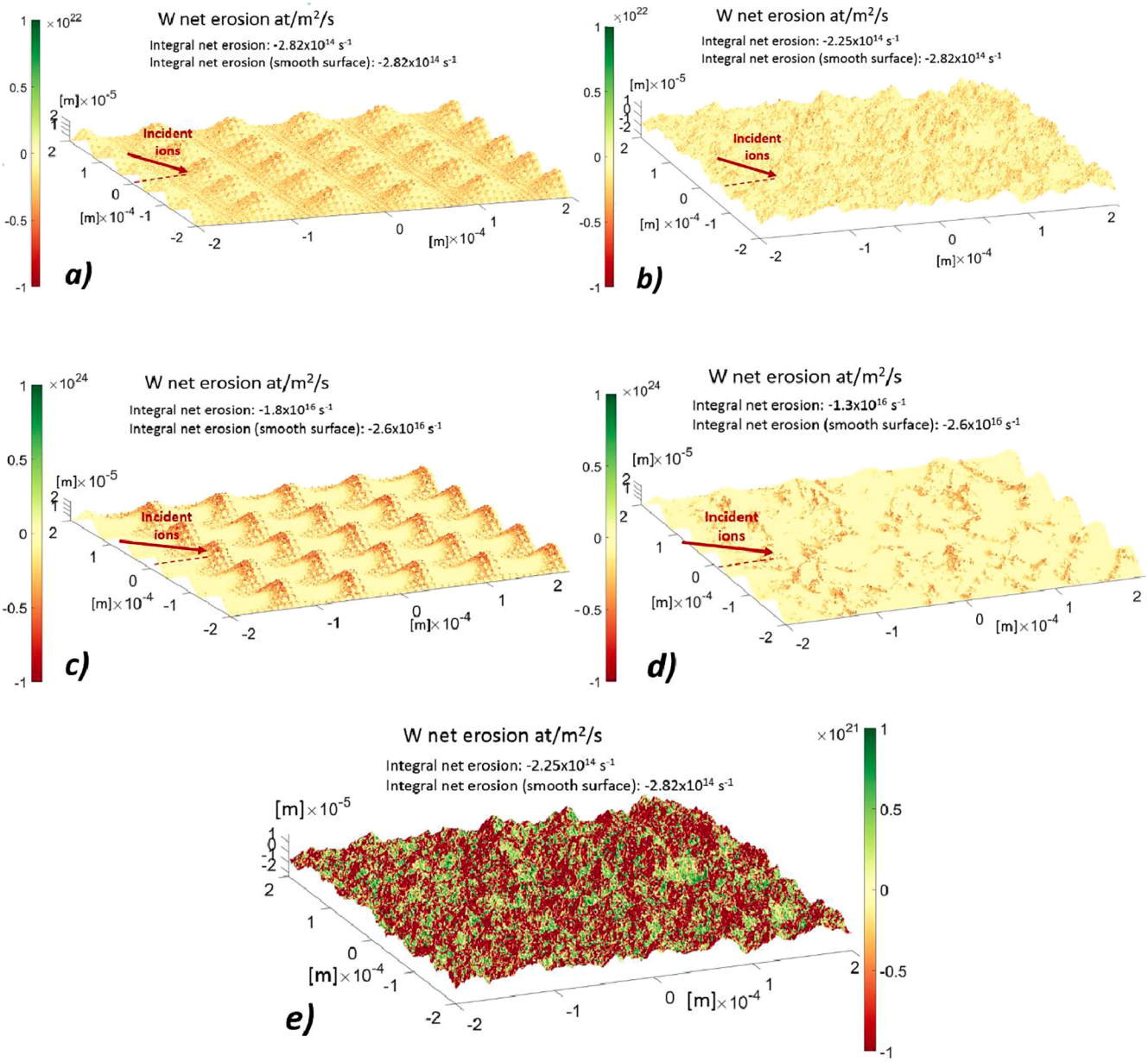

Fig. 8. Net erosion distribution on the rough surface for Tile 5 of the JET-ILW divertor. a) Cosine peaks, inter-ELM conditions; b) randomly-formed topography, inter-ELM conditions; c) cosine peaks, intra-ELM conditions; d) randomly-formed topography, intra-ELM conditions; e) randomly-formed topography, inter-ELM conditions (color-bar scaled on the deposition values).

at the JET-ILW Tile 5/Tile 6 under more realistic shadowing assumptions. According to ERO2.0 simulations, net erosion values for the rough surface corresponding to Tile 6 are up to 50% lower than that of Tile 5 (smooth surface). Furthermore, preferential erosion occurs at plasma-wetted 10 μm-scale "peaks" of the surface, while deposition occurs inside the "valleys". Both results go in line with the experimental findings. Even though in some of considered cases surface roughness have shown to affect the angular distribution of sputtered particles, it is not likely to increase their penetration length into the plasma, since the surface roughness decreases this value due to the more oblique angular distribution of sputtered particles.

Declaration of Competing Interest

The authors declare that they have no known competing financial interests or personal relationships that could have appeared to influence the work reported in this paper.

Acknowledgments

The authors would like to acknowledge Dr. A. Widdowson and Dr. A. Baron-Wiechec for providing information concerning the JET-ILW Tile 5 and Tile 6 surface roughness. The authors gratefully acknowledge the computing time granted through JARA on the supercomputer JURECA at Forschungszentrum Jülich. This work has been carried out within the framework of the EUROfusion Consortium and has received funding from the Euratom research and training programme 2014-2018 and 2019-2020 under grant agreement No 633053. The views and opinions expressed herein do not necessarily reflect those of the European Commission.

References

[1] S. Brezinsek, J. Nucl. Mater. 463 (2015) 11–21.
[2] M. Mayer, et al., J. Nucl. Mater. 363 (2007) 101–106.
[3] A. Hakola, et al., Phys. Scripta T159 (2014) 014027.

[4] A. Kreter, et al., Plasma Phys. Controlled Fusion 50 (9) (2008), 095008.
[5] K. Schmid, M. Mayer, C. Adelhelm, et al., Nucl. Fusion 50 (2010), 105004.
[6] A. Eksaeva, et al., Phys. Scr. T170 (2017), 014051.
[7] J.N. Brooks, et al., No. CONF-900505–10. Argonne National Lab., 1990.
[8] S. Quan, et al., Contrib. Plasma Phys. 57 (8) (2017) 329–335.
[9] R.H. Cohen, et al., Contrib. Plasma Phys. 40 (3-4) (2000) 456–470.
[10] S. Dai, et al., J. Nucl. Mater. 463 (2015) 372–376.
[11] P.R. Arredondo, SIESTA: A new ion source setup and its application to erosion studies on first-wall materials for fusion reactors. 2019.
[12] J. Romazanov, et al., Nucl. Mater. Energy 18 (2019) 331–338.
[13] A. Kirschner, et al., Contrib. Plasma Phys. 56 (6-8) (2016) 622–627.
[14] D. Borodin, et al., Nucl. Mater. Energy 19 (2019) 510–515.
[15] A. Eksaeva, et al., Nucl. Mater. Energy 19 (2019) 13–18.
[16] A. Eksaeva, et al., Phys. Scripta T171 (2020) 014057.
[17] R. Garcıa, et al., Surf. Sci. Rep. 47 (6-8) (2002) 197–301.
[18] D. Borodin, et al., J. Nucl. Mater. 415 (2011) S219.
[19] Mutzke, A., et al. "SDTrimSP Version 6.00." (2019).
[20] Behrisch, R., et al. Vol. 110. Springer Science & Business Media, 2007.
[21] A. Kreter, et al., Fusion Sci. Technol. 68 (1) (2015) 8–14.
[22] D. Dellasega, et al., J. Appl. Phys. 112 (2012), 084328, https://doi.org/10.1063/1.4761842.
[23] Eksaeva A. "Effect of surface morphology on erosion of metallic plasma-facing materials modelled with the 3D Monte-Carlo code ERO". PhD thesis (2020).
[24] Mayer, M., et al. Preprint: 2018 IAEA Fusion Energy Conference, Gandhinagar [EX/P1-15] 2018.
[25] Widdowson A. and Baron-Wiechec A. - information on surface state of Tiles 5 and 6 of JET-ILW (CCFE, Culham, UK, personal connection).
[26] M. Mayer, et al., Phys. Scr. 170 (2017).
[27] A. Kirschner, et al., Nucl. Mater. Energy 18 (2019) 239–244.
[28] I.E. Borodkina, et al., Phys. Proc. 71 (2015) 25–29.
[29] Borodkina, I., et al. Journal of Physics: Conference Series. Vol. 748. No. 1. IOP Publishing, 2016.
[30] S. Brezinsek, et al., Nucl. Fusion 59 (9) (2019).